

Evolution of Plumage Patterns in a Pattern Morphospace: A Phylogenetic Analysis of Melanerpine Woodpeckers

Monica L. Carlson* and Mary Caswell Stoddard

Department of Ecology and Evolutionary Biology, Princeton University, Princeton, New Jersey 08544

Submitted May 13, 2022; Accepted June 12, 2023; Electronically published November 14, 2023

Online enhancements: supplemental PDF.

ABSTRACT: Plumage patterns of melanerpine (*Melanerpes-sphyrapicus*) woodpeckers are strikingly diverse. Understanding the evolution and function of this diversity is challenging because of the difficulty of quantifying plumage patterns. We use a three-dimensional space to characterize the evolution of melanerpine achromatic plumage patterns. The axes of the space are three pattern features (spatial frequency, orientation, and contrast) quantified using two-dimensional fast Fourier transformation of museum specimen images. Mapping plumage in pattern space reveals differences in how species and subclades occupy the space. To quantify these differences, we derive two new measures of pattern: pattern diversity (diversity across plumage patches within a species) and pattern uniqueness (divergence of patterns from those of other species). We estimate that the melanerpine ancestor had mottled plumage and find that pattern traits across patches and subclades evolve at different rates. We also find that smaller species are more likely to display horizontal face patterning. We promote pattern spaces as powerful tools for investigating animal pattern evolution.

Keywords: plumage pattern evolution, animal patterns, pattern morphospace, Fourier analysis, melanerpine woodpecker, *Melanerpes*.

Introduction

Complex spatial patterns in animal integuments serve important functions in social signaling as well as predator avoidance (Endler 1983; Ruxton et al. 2004). In birds, complex plumage patterns, such as bars, streaks, and spots, are created by the regulation of melanin deposition both within and across feathers and are typically composed of black, brown, and/or white plumage (Prum and Williamson 2002; Galván et al. 2017; Inaba and Chuong 2020). Because of their multidimensional nature, plumage patterns are difficult to describe and quantify. A single metric cannot describe the difference between fine horizontal barring and coarse spots, for example. For this reason, studies of plum-

age pattern evolution have historically relied on qualitative judgments by human observers to define and classify patterns, potentially leading to biased results. Furthermore, our ability to understand the evolution of plumage patterns has been stymied by the lack of a quantitative theoretical framework for analyzing complex spatial patterns (Rosenthal 2007; Stoddard and Osorio 2019).

To address this gap, a “pattern space” has been suggested as a tool for studying animal patterns (Stoddard and Osorio 2019; Mason and Bowie 2020), analogous to color spaces that are currently used to study animal coloration (Endler and Mielke 2005; Stoddard and Prum 2008; Kemp et al. 2015; Renoult et al. 2015). In a pattern space, biologically relevant pattern features, such as spatial frequency, orientation, and contrast, serve as axes in the multidimensional space (Stoddard and Osorio 2019). Depending on the question and the patterns being analyzed, the space may consist of fewer or additional pattern dimensions. Pattern spaces hold promise for advancing our understanding of the ecology and evolution of animal patterns because they (1) can be used to analyze pattern variation and evolution quantitatively within an ecologically relevant framework, (2) enable development of novel metrics for analyzing animal patterns, and (3) allow for detailed investigations of pattern function.

The tools for building a pattern space have improved significantly over the past century. To eliminate subjectivity in pattern quantification, many researchers have adopted computational methods to investigate aspects of animal patterning (Godfrey et al. 1987; Westmoreland and Kiltie 1996; Stevens and Cuthill 2006; Barbosa et al. 2008; Chiao et al. 2009; Stoddard and Stevens 2010; Endler 2012; Stevens et al. 2014, 2017; Stoddard et al. 2014, 2016, 2016, 2019; Kang et al. 2015; Troscianko and Stevens 2015; Marques et al. 2016; Troscianko et al. 2017, 2021; Belleghem et al. 2018; Miller et al. 2019; Mason and Bowie 2020; van den Berg et al. 2020; Beco et al. 2021; Mason et al. 2021; Nokelainen

* Corresponding author; email: monica.lynn.carlson@gmail.com.

ORCID: Carlson, <https://orcid.org/0000-0003-2924-9822>; Stoddard, <https://orcid.org/0000-0001-8264-3170>.

et al. 2021; Zhou et al. 2021). Recently, several toolboxes for pattern analysis have been developed, such as the mica-Toolbox for ImageJ (Trosciano and Stevens 2015), the patternize package for R (Belleghem et al. 2018), and QCPA for ImageJ (van den Berg et al. 2020). Algorithms used in these toolboxes are typically based on methods that decompose images in a way that resembles image processing in early stages of spatial vision (Stoddard and Osorio 2019). Two-dimensional Fourier transformation, for example, decomposes an image into its sine wave components, from which pattern statistics, such as spatial frequency, orientation, and contrast, can be extracted (Ballard and Brown 1982). Neurobiological studies in a variety of animal taxa, including birds, show that neurons in early visual areas of the brain are tuned to spatial frequency, orientation, and contrast of a stimulus (Hubel and Wiesel 1959, 1968; Pettigrew and Konishi 1976; Porciatti et al. 1989; Lee et al. 1997; Nieder and Wagner 2001; Mazer et al. 2002; Gaffney and Hodos 2003; Liu and Pettigrew 2003; Ghim and Hodos 2006; Baron et al. 2007; Van Hooser 2007; Ng et al. 2010), providing biological grounding for using these pattern attributes as axes in a perceptual pattern space (Stoddard and Osorio 2019). Despite advances in computational methods for pattern quantification, few studies have utilized a quantitatively derived pattern space alongside phylogenetic comparative methods to provide insights into avian plumage pattern evolution.

Here we apply a pattern space to the study of achromatic plumage patterns in the melanerpine (*Melanerpes-Sphyrapicus*) woodpeckers (25 species), a diverse group of woodpeckers inhabiting North, Central, and South America, to characterize and reconstruct the phylogenetic history of plumage pattern evolution in this clade. We chose the melanerpine woodpeckers because they exhibit diverse plumage patterns (fig. 1), including barring, streaking, mottling, and high-contrast “blocky” patterns, as well as uniform, unpatterned plumage (hereafter referred to as “solid” plumage). Here, “barring” refers to striped plumage oriented transverse to the anterior-posterior (A-P) body axis, while “streaking” refers to markings that are oriented parallel to the A-P axis (Riegner 2008). We use the term “mottling” to refer to irregularly shaped spots with no clear orientation. Melanerpine woodpeckers also possess diverse ecologies, behaviors, and life histories. While some melanerpine species could be considered “typical” woodpeckers that scale tree bark to find insects while a mate forages nearby, others include the highly social, cooperatively breeding acorn woodpecker (*Melanerpes formicivorus*), which caches acorns in the open oaklands of California (Winkler and Christie 2015); the omnivorous, solitary Guadeloupe woodpecker (*M. herminieri*), which inhabits island forests (Winkler et al. 2018); cactus-dwelling frugivores, such as the white-fronted woodpecker (*M. cactorum*; Winkler et al. 2013)

and Gila woodpecker (*M. uropygialis*; Winkler and Christie 2013); and the sapsuckers (*Sphyrapicus* spp.), which primarily consume tree phloem and are migratory, an uncommon trait among woodpeckers (Short 1982).

The melanerpine species can be subdivided into five monophyletic subclades (fig. S1; figs. S1–S4 are available online), to which we will refer using the names in Navarro-Sigüenza et al. (2017): (1) members of the “Centurus” subclade span the entire geographic range of the melanerpine clade, possess vastly different body sizes, and all exhibit dorsal barring; (2) the “Tripsurus” subclade primarily consists of small-bodied species with minimal barring that inhabit tropical areas (with the exception of *M. hypopolius*; see below); (3) the “typical Melanerpes” subclade is a highly diverse group in terms of body size, geographic range, foraging and social behaviors, and plumage pattern; (4) the Hispaniolan woodpecker (*M. striatus*), a colonial, large-bodied species with yellow-green and black dorsal barring, comprises a monotypic lineage; and (5) members of the genus *Sphyrapicus*, the small-bodied, migratory sapsuckers, all of which have some degree of mottled plumage and are restricted to temperate regions in North America, comprise a final subclade. Recent phylogenetic studies of the melanerpine woodpeckers are mostly in agreement about the relationships both within and among these subclades (Navarro-Sigüenza et al. 2017; Shakya et al. 2017).

To explore the evolution and diversity of melanerpine woodpecker plumage patterns, we use two-dimensional fast Fourier transformation (2D FFT) to quantify three pattern features (spatial frequency, pattern orientation, and contrast) from standardized, calibrated museum specimen images. Next, we project these features into a three-dimensional space and derive two new measures of pattern: pattern diversity, which represents the extent to which achromatic pattern features differ across plumage patches, and pattern uniqueness, which represents the extent to which a species’ achromatic pattern features differ in comparison to other melanerpines. We also use species’ relative locations in pattern space to derive a measure of plumage pattern variation within melanerpine subclades. We then map measures of pattern (spatial frequency, orientation, contrast, pattern diversity, and pattern uniqueness) onto a molecular phylogeny (Shakya et al. 2017) to examine phylogenetic trends in the evolution of plumage pattern and reconstruct an estimate of the ancestral melanerpine plumage. Finally, we employ phylogenetic generalized least squares (PGLS) regression to test for possible adaptive functions of achromatic plumage patterns in the melanerpine woodpeckers.

Methods

A detailed description of the methods is provided in the supplemental PDF.

Image Data Collection

We studied the achromatic plumage patterns of 25 species in the melanerpine woodpecker genera *Melanerpes* (22 species) and *Sphyrapicus* (3 species). We selected this clade because of its diversity in complex plumage patterns and the availability of a recent, well-supported phylogeny (Shakya et al. 2017). We photographed museum specimens using an ultraviolet-sensitive digital Nikon D7000 camera with a Nikkor 105-mm lens, following published procedures (Stevens et al. 2007; Troschianko and Stevens 2015). In most cases, we were able to photograph five adult male specimens per species from collections at the Academy of Natural Sciences of Drexel University (ANSDU) and the American Museum of Natural History (AMNH). See the supplemental PDF for details and table D1 in the Dryad Digital Repository (<https://doi.org/10.5061/dryad.2rbnzs7qq>; Carlson and Stoddard 2023) for a list of all specimens used.

Avian Visual Modeling

Because the evolution of visual signals is influenced by receivers' perception, we used visual modeling to approximate how woodpecker plumage patches would be perceived by the main receivers of these signals, which we assumed to be birds. See the supplemental PDF for details.

Patch Selection

From each specimen image, we selected a square patch within the following 12 plumage regions (five dorsal, five ventral, and two lateral) in MATLAB (dorsal view: cap [1.1 cm × 1.1 cm], nape [2.3 cm × 2.3 cm], upper back/mantle [2.8 cm × 2.8 cm], middle back/wings [3.4 cm × 3.4 cm], and lower back/wings [2.3 cm × 2.3 cm]; ventral view: chin [1.1 cm × 1.1 cm], throat [1.4 cm × 1.4 cm], chest [2.3 cm × 2.3 cm], belly [2.3 cm × 2.3 cm], and vent [2.3 cm × 2.3 cm]; lateral view: face [3.0 cm × 3.0 cm] and wing [1.8 cm × 1.8 cm]). See figure S2 for an example.

Pattern Quantification

For each plumage patch, we extracted three pattern features: contrast, spatial frequency, and orientation. Figure 2 is a visualization of the methods we used to extract these features. See the supplemental PDF for details.

We combined z -transformed mean spatial frequency, orientation, and contrast to produce a three-dimensional pattern morphospace in which we plotted species averages for each of the 12 plumage patches. For each species, we measured pattern diversity by computing the mean pairwise Euclidean distance between all 12 plumage patches from that species in pattern space. To calculate a species' pattern

uniqueness, we used a patch-by-patch approach: for each of the 12 patches, we computed the mean Euclidean distance of that species' patch (e.g., the face patch) from the same patch in the remaining 24 species. We then calculated overall uniqueness of each species' plumage by taking the mean of these 12 values. To measure pattern variation within each melanerpine subclade, we computed the mean Euclidean distance between analogous patches for the species in each subclade. We refer to this measure as the variation index, similar to the V -index proposed by Marcondes and Brumfield (2020). See the supplemental PDF for more details.

Trait Mapping, Evolutionary Modeling, and Evolutionary Rate Comparisons

For our evolutionary analyses, we used the phylogenetic consensus tree from Shakya et al. (2017) pruned to the melanerpine woodpecker species. To explore how achromatic pattern traits evolve across this phylogeny, we fitted seven different evolutionary models (Brownian motion, Ornstein-Uhlenbeck, early burst, Pagel's δ , Pagel's λ , trend, and white noise) for spatial frequency, orientation, and contrast for three plumage patches of interest (the upper back, chest, and face), as well as for pattern diversity and uniqueness (which encompass all patches), using the function `fitContinuous` in the R package `GEIGER` (Harmon et al. 2008). We chose to compare evolutionary rates across these patches because these patches are hypothesized to be used in different ecological and behavioral contexts, and therefore their evolution is likely to show different trends.

To compare rates of pattern orientation evolution across plumage patches, we used the `compare.multi.evol.rates` function in the R package `geomorph` (Adams et al. 2021; Baken et al. 2021). We applied this function to pattern orientation in the upper back, chest, and face and compared each rate ratio (upper back to chest, upper back to face, chest to face) with those obtained from 1,000 simulated trees to determine significance of the differences in rates.

We also tested for evolutionary rate (σ^2) differences in spatial frequency, orientation, and contrast in the "typical *Melanerpes*" subclade relative to the rest of the tree using a similar function, `compare.evol.rates` in the R package `geomorph` (Adams et al. 2021; Baken et al. 2021). We chose the "typical *Melanerpes*" subclade for this comparison because of its notable diversity in both plumage and ecology. See the supplemental PDF for more details.

Ancestral State Estimation

We applied the function `ace` in the R package `ape` (Paradis and Schliep 2019) in combination with the tree transformation function (`lambdaTree`) in the R package



Figure 1: Adult male plumages of *Melanerpes* and *Sphyrapicus* woodpeckers. A, Golden-fronted woodpecker, *Melanerpes aurifrons* (by Outrigger [2006–2009], CC BY-SA 3.0/cropped). B, White-fronted woodpecker, *Melanerpes cactorum* (by Karina Diarte, CC BY-NC-SA 2.0/cropped). C, White woodpecker, *Melanerpes candidus* (by Cláudio Timm, CC BY-NC-SA 2.0/cropped). D, Red-bellied woodpecker, *Melanerpes carolinus* (by TheGreenHeron, CC BY-NC 2.0/cropped). E, Golden-naped woodpecker, *Melanerpes chrysauchen* (© Daniel Martinez, ML142698991/cropped). F, Golden-cheeked woodpecker, *Melanerpes chrysogenys* (© Nigel Voaden, ML46659301/cropped). G, Yellow-tufted woodpecker, *Melanerpes cruentatus* (© Phillip Edwards, ML204878711/cropped). H, Red-headed woodpecker, *Melanerpes erythrocephalus* (by jerryoldenettel, CC BY-NC-SA 2.0/cropped). I, Yellow-fronted woodpecker, *Melanerpes flavifrons* (by Cláudio Timm, CC BY-NC-SA 2.0/cropped). J, Acorn woodpecker, *Melanerpes formicivorus* (by jerryoldenettel, CC BY-NC-SA 2.0). K, Guadeloupe woodpecker, *Melanerpes herminieri* (by thoba69, CC BY-NC-SA 2.0/cropped). L, Hoffman’s woodpecker, *Melanerpes hoffmannii* (by Muchaxo, CC BY-NC-ND 2.0/cropped). M, Gray-breasted woodpecker, *Melanerpes hypopolius* (by Sergey Yeliseev, CC BY-NC-ND 2.0/cropped). N, Lewis’s woodpecker, *Melanerpes lewis* (by wackybadger, CC BY-SA 2.0/cropped). O, Puerto Rican woodpecker, *Melanerpes portoricensis* (by Drriss & Marrionn, CC BY-NC-SA 2.0/cropped). P, Black-cheeked woodpecker, *Melanerpes pucherani* (by felixú, CC BY-SA 2.0/cropped). Q, Yucatan woodpecker, *Melanerpes pygmaeus* (© Angel Fernando Castillo Cime, ML196772131/cropped). R, Jamaican woodpecker,

GEIGER (Harmon et al. 2008) to estimate the ancestral states for spatial frequency, orientation, and contrast for each of the 12 plumage patches using maximum likelihood (Felsenstein 1973; Schluter et al. 1997).

Ecological Data Collection

For body mass data, we used average male body mass for each species (Dunning 2008). To quantify all other ecological data, we scored written data from species descriptions from *Handbook of the Birds of the World Alive*. See the supplemental PDF and table D2 in the Dryad Digital Repository (<https://doi.org/10.5061/dryad.2rbnzs7qq>; Carlson and Stoddard 2023) for details.

Testing for Ecological Correlates of Plumage Pattern

To test for drivers of plumage pattern, we ran PGLS multiple linear regression models with pattern metrics as outcome variables and ecological factors as predictor variables. See the supplemental PDF for details.

Results

Species' Plumage Patterns in Pattern Space

To visualize where types of plumage patterns fall in pattern morphospace, we created plots of individual plumage patches. Figure 3 shows pattern space plots from the upper-back patch for all species, with points representing species averages. The three-dimensional morphospace is shown as two two-dimensional graphs to better visualize variation along the axes. The letters inside circles represent species (fig. 1), and circle color represents the melanerpe subclade to which each species belongs (fig. S1). Species averages for each pattern trait (spatial frequency, orientation, and contrast) for all 12 plumage patches, as well as species averages for pattern diversity and uniqueness, are included in table D3 in the Dryad Digital Repository (<https://doi.org/10.5061/dryad.2rbnzs7qq>; Carlson and Stoddard 2023).

This morphospace clearly captures pattern variation, demonstrating the effectiveness of 2D FFT at quantifying plumage patterns: upper-back patch images cluster together based on visual similarity, with barred-back species, streaked-back species, and solid-back species each forming rela-

tively isolated clusters (fig. 3). Mottled-back species tend to group with the streaked-back species, although the orientation values of the mottled-back species fall closer to zero (fig. 3A). Most of the barred-back species occupy the right-hand corner of both plots, corresponding to high spatial frequency (i.e., fine patterning), high contrast, and horizontal orientation (fig. 3). In comparison, streaked-back species have lower spatial frequencies, similar levels of contrast, and vertically oriented patterning (fig. 3). Finally, solid-backed species occupy the lower left-hand corner of both plots, corresponding to low spatial frequencies, low contrast, and orientation values that are closer to zero (fig. 3). The orientation values of solid patches fall below zero (i.e., more vertical) because of the primarily vertical orientation of feathers that are visible in the specimen images.

To visualize how plumage pattern varies between species, we created species-specific pattern space plots representing all 12 plumage patches. Three example species are shown in figure 4.

The species-specific pattern space plots show substantial pattern variation among plumages of melanerpine woodpeckers. The point cloud of the acorn woodpecker, *Melanerpes formicivorus* (fig. 4A), a species with bold, blocky plumage patches and fine ventral streaking, occupies areas of the pattern space corresponding to both vertical and horizontal orientation information, low and high spatial frequency, and low and high contrast. The point cloud of the Guadeloupe woodpecker, *M. herminieri* (fig. 4B), a species with primarily solid plumage, is restricted to areas of the space corresponding to lower spatial frequencies, very low contrast, and a smaller range of pattern orientations. It should be noted that, although this species appears to be unpatterned, specular reflections from the texture of the feather barbs and rachises register as patterns in the 2D FFT analysis, and therefore the ranges of spatial frequency and orientation are wider than one might expect. The point cloud of the red-bellied woodpecker, *M. carolinus* (fig. 4C), a species with black and white dorsal barring, extends into areas in pattern space corresponding to high spatial frequency and high horizontal pattern information because of the fine transverse barring in the dorsal plumage, while its solid ventral plumage is represented by points in the region of pattern space corresponding to low spatial frequency, low contrast, and less horizontally oriented patterning.

Melanerpes radiolatus (by nickathanas, CC BY-NC-SA 2.0/cropped). S, Red-crowned woodpecker, *Melanerpes rubricapillus* (by Martingloor, CC BY-SA 4.0/cropped). T, Hispaniolan woodpecker, *Melanerpes striatus* (© Dubi Shapiro, ML205133391/square background added). U, West Indian woodpecker, *Melanerpes superciliosus* (© Dubi Shapiro, ML205135651/cropped). V, Gila woodpecker, *Melanerpes uropygialis* (by MPF, CC BY-SA 2.0/cropped). W, Red-breasted sapsucker, *Sphyrapicus ruber* (by Michael Gabelmann, CC BY-NC 2.0/cropped). X, Williamson's sapsucker, *Sphyrapicus thyroideus* (by K Schneider, CC BY-NC 2.0/cropped). Y, Yellow-bellied sapsucker, *Sphyrapicus varius* (by Howcheng, CC BY-SA 2.0/cropped). Images E–G, Q, T, and U provided by the Macaulay Library at the Cornell Lab of Ornithology. All other images licensed by Creative Commons.

Representation in Pattern Space

Extraction of Pattern Features

Image Processing

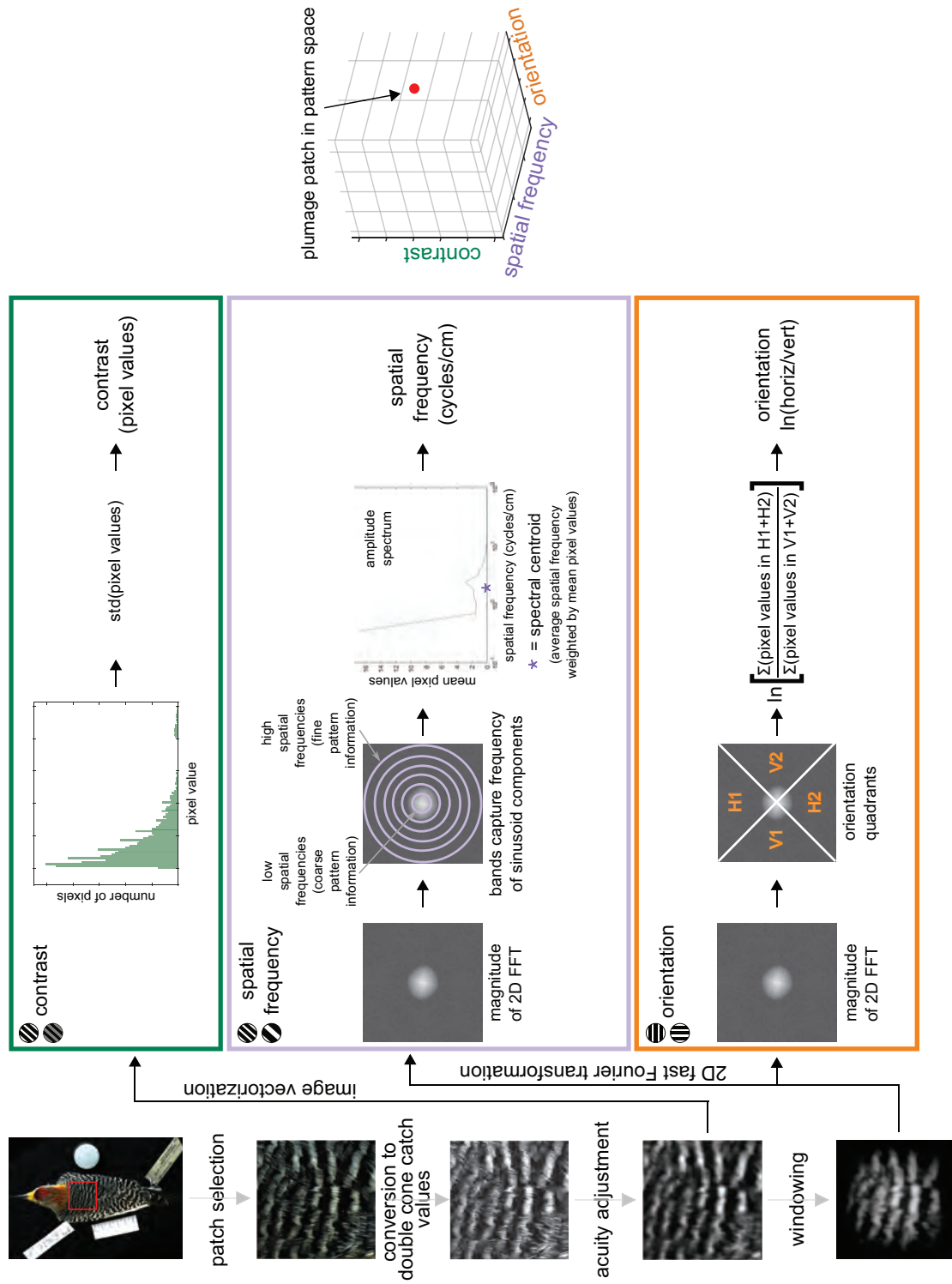


Figure 2: Visualization of pattern analysis process. Plumage patch regions are selected from standardized, calibrated RAW images of museum specimens, followed by avian visual modeling (conversion to double-cone catch values and adjustment for signal receiver acuity). Contrast, spatial frequency, and orientation are subsequently measured from the acuity-adjusted, double-cone image. 2D FFT = two-dimensional fast Fourier transformation.

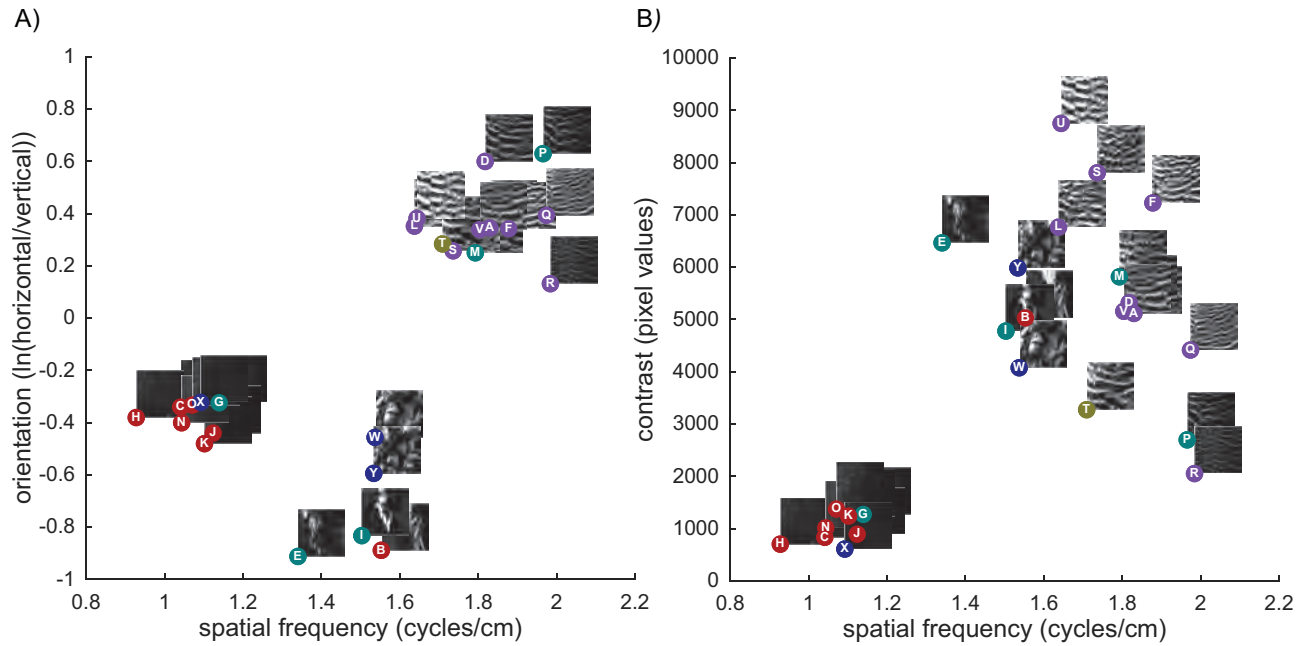


Figure 3: Pattern space plots for the upper-back (mantle) plumage patch. Plots are shown in two dimensions for visualization. Points represent species averages. Spatial frequency (x-axis in both plots) is measured as the spectral centroid of the amplitude spectrum for that patch. For orientation (A), positive values represent more horizontal patterning, while negative values represent more vertical patterning. Contrast (B) is measured as the standard deviation of the pixel values in the acuity-adjusted, double-cone plumage patch image. Thumbnails of an example specimen from each species are offset above and to the right of each point. Letters within circles refer to species; see figure 1. Colors of circles refer to subclades within *Melanerpes-Sphyrapicus*; see figure 5D.

To visualize variation in pattern diversity across the clade, we mapped pattern diversity values onto the melanerpine phylogenetic tree (fig. 5D, filled circles). Acorn woodpecker (*M. formicivorus*) had the highest pattern diversity, while Guadeloupe woodpecker (*M. herminieri*) had the lowest. Pattern space plots and images for both of these species are shown in figure 4. Members of the subclade “Centurus,” the barred-back subclade, all have moderately high levels of pattern diversity owing to vastly different plumage on the dorsum (fine barring) versus the venter (primarily solid; fig. 5D). The subclade referred to as “typical *Melanerpes*” shows a great degree of variation in terms of pattern diversity (fig. 5D), containing species with very low pattern diversity (e.g., *M. herminieri* and *M. portoricensis*) as well as some with very high pattern diversity (e.g., *M. formicivorus*). The “typical *Melanerpes*” members red-headed woodpecker (*M. erythrocephalus*) and white woodpecker (*M. candidus*) also have high levels of pattern diversity, despite a lack of barring, streaking, or other fine patterning (figs. 1, 5D). These species achieve a high level of pattern diversity with vast spans in the contrast and orientation dimensions.

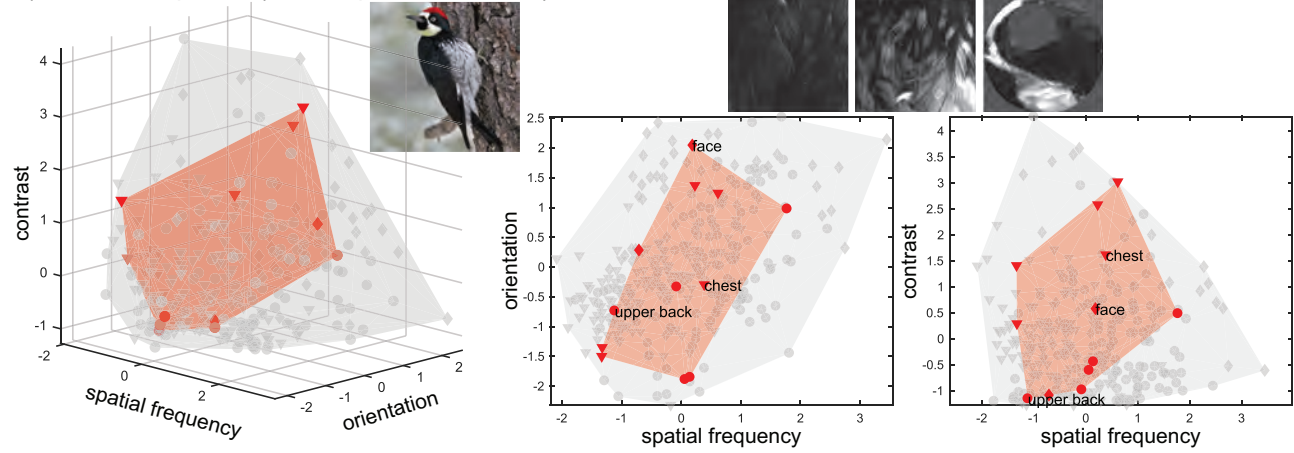
We plotted pattern uniqueness values onto the phylogeny to visualize how this trait is distributed across the tree (fig. 5D, open circles). White woodpecker (*M. candidus*),

acorn woodpecker (*M. formicivorus*), and Lewis’s woodpecker (*M. lewis*) ranked as the three most unique species of the melanerpine woodpeckers, which aligns with a visual assessment (fig. 1).

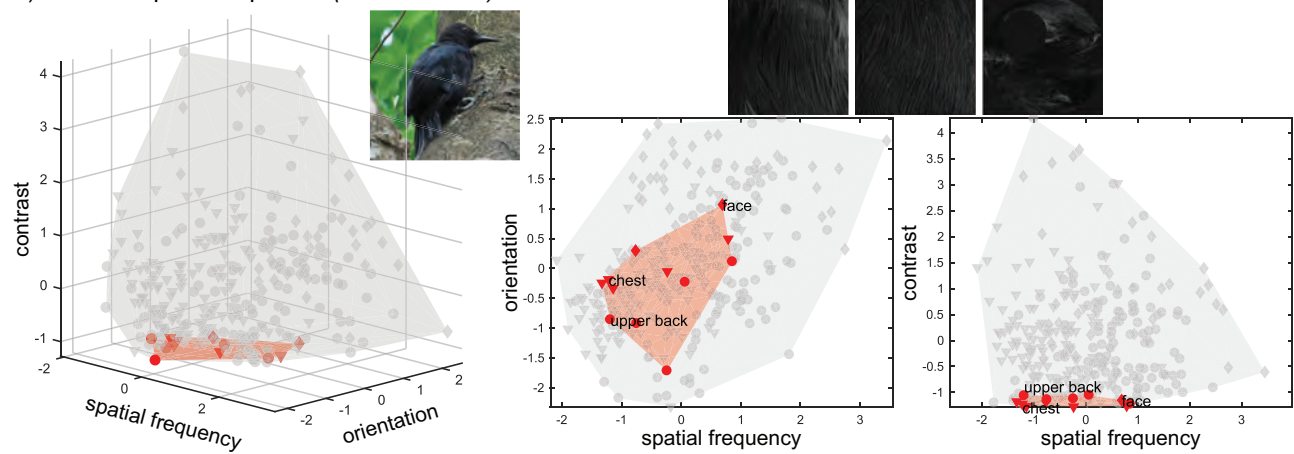
To visualize how phylogenetic subclades within the melanerpine woodpeckers differ in their occupation of pattern space, we plotted convex hulls from the points representing the plumage patches of all of the species within a subclade in a single three-dimensional pattern space plot (fig. 5A). Two-dimensional plots of the same data are shown in figure 5B and 5C for ease of visualization. Convex hull colors represent the five subclades denoted in figure 5D. There is significant overlap in the subclade convex hull volumes, but some subclades extend beyond the area of overlap. For example, the convex hull representing the “Centurus” subclade (magenta), whose species all exhibit dorsal barring, extends farthest into the area of pattern space representing high spatial frequency (i.e., fine patterning) and horizontal orientation values.

Figure 5E–5L depicts the extent to which the convex hulls of each species (shown in a different shade of the subclade color) overlap each other; the outline represents the convex hull of the entire subclade. Results of our quantitative analysis of within-subclade variation revealed that the “typical *Melanerpes*” subclade (fig. 5I, 5J) had the

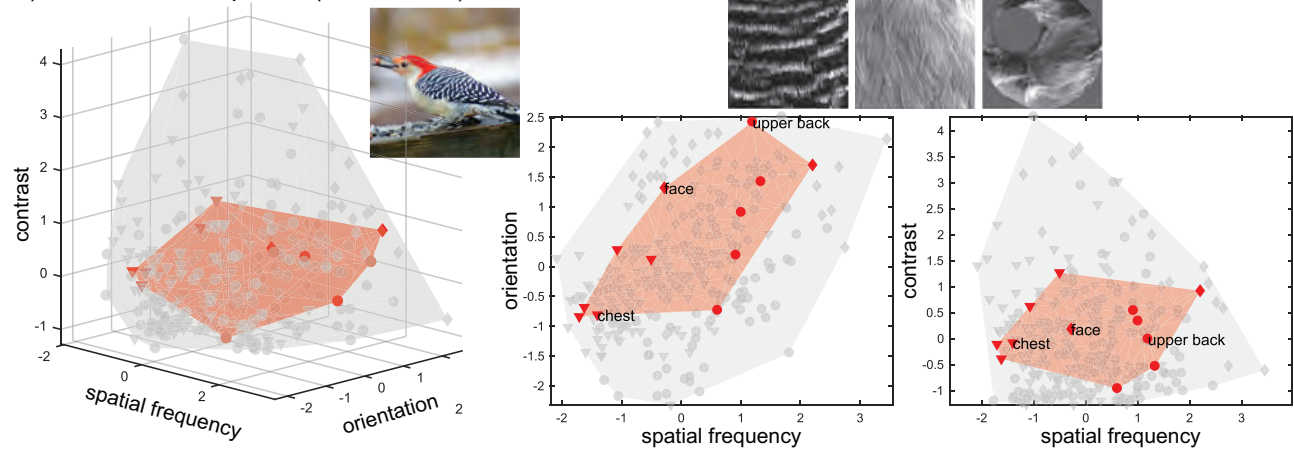
A) acorn woodpecker (*Melanerpes formicivorus*)



B) Guadeloupe woodpecker (*M. herminieri*)



C) red-bellied woodpecker (*M. carolinus*)



◆ lateral patch, example species ◆ lateral patch, other Melanerpe species
▼ ventral patch, example species ▼ ventral patch, other Melanerpe species
● dorsal patch, example species ● dorsal patch, other Melanerpe species

Figure 4: Diversity of pattern space occupancy illustrated by three example melanerpine species. *A*, Acorn woodpecker (*Melanerpes formicivorus*). *B*, Guadeloupe woodpecker (*Melanerpes herminieri*). *C*, Red-bellied woodpecker (*Melanerpes carolinus*). All points represent species averages; pattern metrics are z-transformed. Red points represent locations of the example species' 12 plumage patches in pattern space; gray points represent the remaining 24 species' plumage patch locations. Convex hulls of the example species (light red) and all species (light gray) are shown for comparison. Diamonds represent lateral patches, triangles represent ventral patches, and circles represent dorsal patches. Positive orientation values represent more horizontal patterning, while negative values represent more vertical patterning. Examples of the upper-back, chest, and face patches for each species are shown above the two-dimensional pattern space plots. Woodpecker photo credits: *A*, Acorn woodpecker, *M. formicivorus* (by jerryoldenettel, CC BY-NC-SA 2.0). *B*, Guadeloupe woodpecker, *M. herminieri* (by thoba69, CC BY-NC-SA 2.0/cropped). *C*, Red-bellied woodpecker, *M. carolinus* (by TheGreenHeron, CC BY-NC 2.0/cropped).

highest variation index (2.44) of the four subclades, which is in line with a qualitative visual assessment of this subclade: each species displays a truly unique plumage pattern (figs. 1, 5D). “Tripsurus” had the second-highest variation index (1.88), reflecting a relatively diverse group including barred-backed, streak-backed, and solid-backed species (figs. 1, 5D). The “Centurus” subclade had a variation index of 1.45, reflecting less variation than the previous two subclades but more variation than the mottled *Sphyrapicus* subclade, which had a variation index of 1.37. A visual assessment of “Centurus” and *Sphyrapicus* (figs. 1, 5D) confirms that these subclades display less plumage pattern heterogeneity across species than the “typical Melanerpes” and “Tripsurus” subclades. We note that the extent of convex hull overlap has also been used to quantify plumage variation within taxonomic clades (Marcondes and Brumfield 2020). For comparison, we computed within-subclade variation using convex hull overlap and found that the results showed the same pattern as the Euclidean distance-based measure. We also note that some of the variation within each subclade may be due to the number of species in each subclade (e.g., *Sphyrapicus* has the smallest variation as well as the smallest number of species), but it is not possible to determine the extent to which subclade size is affecting these measures with a sample size of only four subclades.

Evolution of Plumage Patterns

Overall, evolutionary model comparison revealed that there was no single best model for pattern evolution in the three patches of interest (upper back, chest, and face), as measured by corrected Akaike information criterion (AICc; i.e., the model with the lowest AICc value was within 4 AICc units of the next-best model); the same was true for pattern diversity and pattern uniqueness. See table S1 (tables S1–S7 are available online) for AICc values and maximum likelihood parameter estimates for all models tested.

Comparing rates of pattern evolution across patches (fig. 6A) revealed that pattern orientation in the upper back evolves more quickly than in the face (rate ratio = 9.06, effect size (z) = 2.63, P = .001) and chest (rate ratio = 4.31, effect size (z) = 2.38, P = .001); rates of pattern orientation evolution in the face and chest did not significantly differ from one another (rate ratio = 2.10, effect size (z) = 1.54, P = .07). Figure S3B shows pattern orientation in the three focal patches mapped onto the melanerpine phylogeny. Branch colors at the nodes of the tree (fig. S3B) represent estimates of ancestral pattern trait states calculated using Felsenstein’s rerooting algorithm (Felsenstein 1985) under a Brownian motion model of evolution.

In addition to comparing achromatic pattern evolution between patches, we compared rates of phenotypic evo-

lution between the “typical Melanerpes” subclade and the remaining species in the melanerpine clade (fig. 6B). Figure 6B shows that pattern orientation (rate ratio = 8.50, effect size (z) = 2.28, P = .003) and contrast (rate ratio = 3.83, effect size (z) = 1.70, P = .04), but not spatial frequency (rate ratio = 1.11, effect size (z) = -1.22, P = .87), evolve at significantly different rates in the “typical Melanerpes” compared with the rest of the tree. Figure S3C shows the evolution of the three pattern metrics averaged across the entire plumage (i.e., all 12 patches) of each species. Branch colors at the nodes of the tree represent estimates of ancestral pattern trait states calculated using Felsenstein’s rerooting algorithm (Felsenstein 1985) under a Brownian motion model of evolution. This whole-body analysis illustrates how the “gestalt” plumage patterns evolve across the tree (fig. S3C).

Ancestral State Estimation

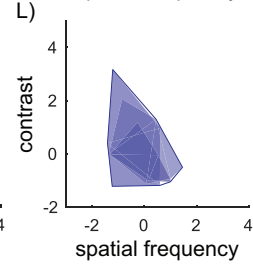
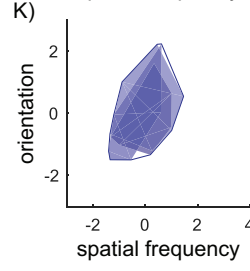
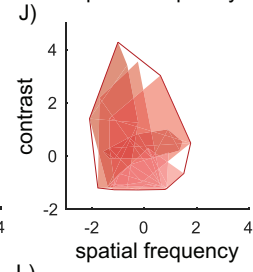
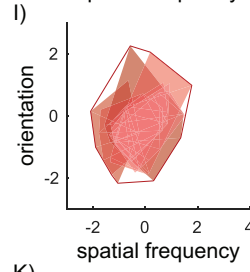
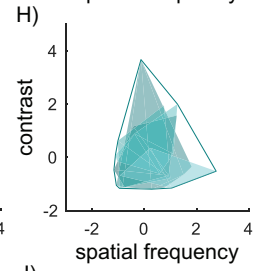
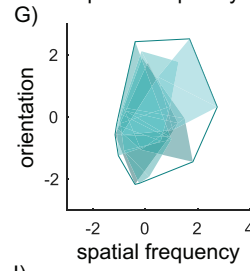
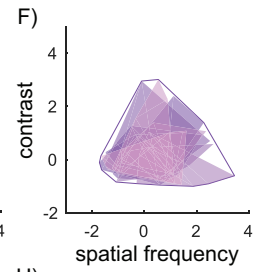
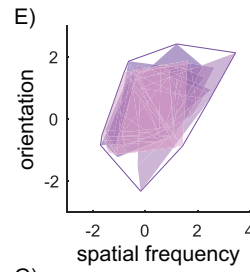
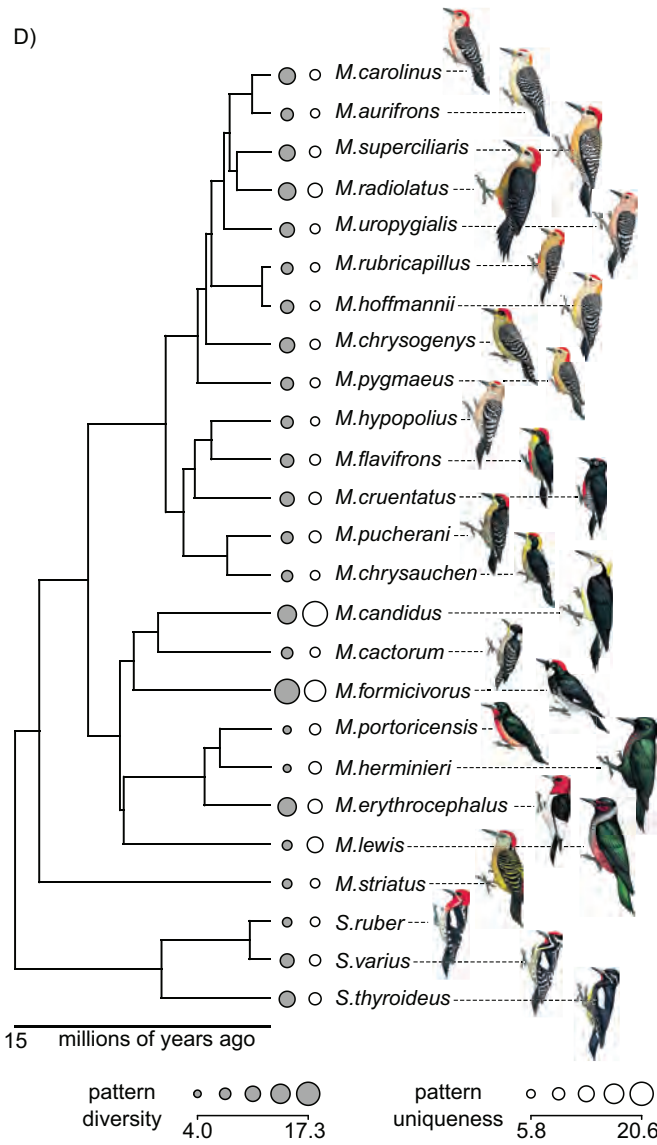
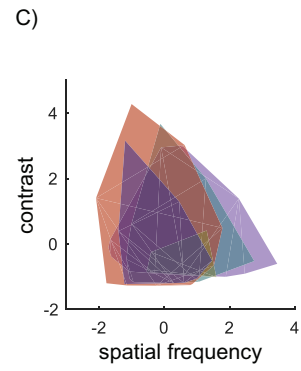
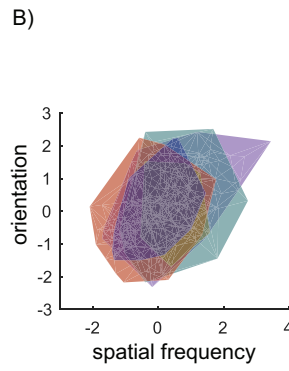
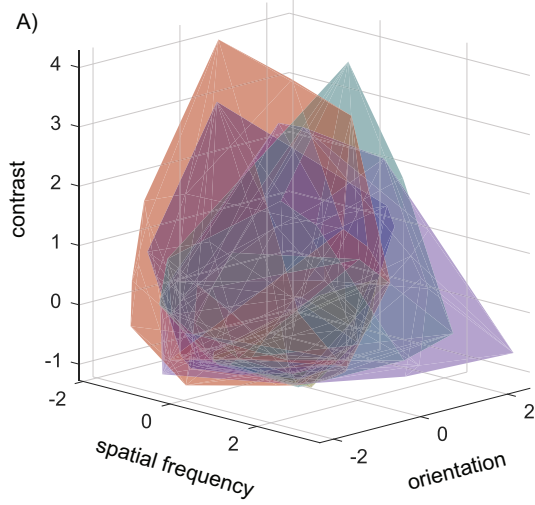
According to our estimates, the ancestor of the entire melanerpine clade most likely had mottled, low-contrast dorsal and lateral wing plumage, solid ventral plumage, and a face with a broad eye stripe. See table S2 for ancestral state estimates of spatial frequency, orientation, and contrast for each of the 12 plumage patches. According to our estimations, it seems unlikely that the ancestor of the melanerpine woodpeckers displayed fine dorsal barring, implying that dorsal barring independently evolved in the “Centurus” subclade and in the gray-backed woodpecker (*M. hypopolius*), black-cheeked woodpecker (*M. pucherani*), and Hispaniolan woodpecker (*M. striatus*).

Ecological Correlates of Plumage Pattern

Results of the multiple linear regression models that we used to test for relationships between ecological variables and pattern features are shown in table S3. Of the 10 models we tested, only the regression model with face orientation as the outcome variable was significant ($R^2_{\text{pred}} = 0.70$, $F_{23,16} = 6.82$, $P < .001$) after correcting for false discovery rate (Benjamini and Hochberg 1995). Within this significant model, we found that average male body mass was a significant predictor of face orientation ($\beta = -0.30$, $P < .01$; table S4): smaller species have more horizontally oriented facial patterning. Sociality was close to significant with a small effect size ($\beta = 0.13$, $P = .05$; table S4): social species trend toward having more horizontally oriented facial patterning. See table S5 for results of all PGLS analyses performed.

Discussion

In our analysis of plumage pattern evolution in the melanerpine woodpeckers, we have shown how applying quantitative



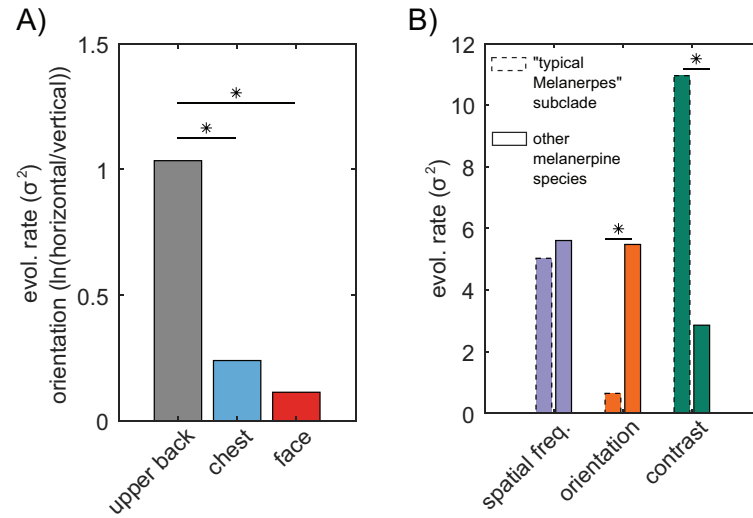


Figure 6: Pattern evolves at different rates across plumage patches and in different subclades. *A*, Pattern orientation ($\ln(\text{horizontal/vertical})$) of upper back evolves significantly faster than in the face or chest. *B*, In the “typical *Melanerpes*” subclade, pattern orientation evolves more slowly and contrast evolves more quickly relative to the rest of the melanerpine tree. Evolutionary rate comparisons were computed using the `compare.evol.rates` and `compare.multi.evol.rates` functions in the R package `geomorph` (Adams et al. 2021; Baken et al. 2021). Colors of bars refer to colors used in mapped trees shown in figure S3.

pattern analysis tools to study visually complex traits allows for a new understanding of how pattern evolves in a multidimensional pattern space. Results from our study provide insights into the evolutionary history of plumage pattern in the *Melanerpes-Sphyrapicus* woodpeckers. In addition, we have used the concept of a pattern space to generate two new measures of pattern, pattern diversity and pattern uniqueness, that can be used to quantify pattern variation both within and across species, as well as among subclades. Furthermore, we have demonstrated how pattern analyses at different spatial scales—entire plumage, plumage view (e.g., dorsal, ventral, or lateral), and plumage patch—provide a holistic understanding of the evolution and function of plumage patterns. Our quantitative measurement of patterns, based on what we know about the biology of visual pattern perception in animals, has allowed us to explore relationships between plumage patterns and ecological variables. The analytical framework and visualization methods we have developed will foster future comparative research investigating the evolution and function of complex spatial patterns in animals.

Biological Relevance of Pattern Space Axes

Stoddard and Osorio (2019) provide an overview of biological spatial vision and its similarities to the computational approaches used to model visual processing. Spatial filtering (i.e., breaking down a pattern into different spatial frequencies) is likely to be a fundamental feature of animal spatial vision, and there is strong evidence that many animals are sensitive to variation in contrast and orientation. Like color spaces, pattern spaces fall short of replicating the visual experience of the animal receiver. Instead, pattern spaces are intended to encode natural patterns in a simple way that is informed by biologically realistic parameters.

The pattern attributes we selected—spatial frequency, orientation, and contrast—as the axes for our woodpecker plumage pattern space analysis are grounded in previous work on visual perception of pattern in human and nonhuman animals, including birds. In several avian species (e.g., American kestrel [*Falco sparverius*], barn owl [*Tyto alba*], Japanese quail [*Coturnix japonica*], pigeons [*Columba livia*], European starling [*Sturnus vulgaris*], red-bellied

Figure 5: Pattern space occupancy of all 12 plumage patches from each of the 25 melanerpine species colored by subclade. *A*, Convex hulls of each melanerpine subclade; colors refer to subclades in *D*. *B*, *C*, Same convex hulls plotted in two dimensions. *D*, Pattern diversity (filled circles) and uniqueness (open circles) plotted on the melanerpine phylogenetic tree; colored bars to the right represent subclades (Navarro-Sigüenza et al. 2017); values in scale bar and size of circles calculated as $e^{(\text{trait value})}$ to emphasize interspecific differences. *E–L*, Convex hulls representing pattern space occupancy of each species within each subclade; outline represents the convex hull of the entire subclade; each species is shown in a different shade of the corresponding subclade color; monotypic subclade containing *Melanerpes striatus* not shown. Phylogenetic tree (*D*) built from data from Shakya et al. (2017) and created using the `dotTree` function in the `phytools` R package (Revell 2012); species images (shown to approximate scale) reproduced with permission from Lynx Edicions.

woodpecker [*Melanerpes carolinus*], and little owl [*Athene noctua*]), neurons in the retina respond to changes in contrast as well as spatial frequency of patterns (Porciatti et al. 1989; Lee et al. 1997; Gaffney and Hodos 2003; Ghim and Hodos 2006). In addition, neurons in an area of the avian brain known as the visual “Wulst,” which possesses structure, connectivity, and function homologous to the primary visual cortex in mammals known as area V1 (Medina and Reiner 2000), are sensitive to pattern orientation in burrowing owls (*Athene cunicularia*), barn owls (*T. alba*), and pigeons (*C. livia*; Pettigrew and Konishi 1976; Nieder and Wagner 2001; Liu and Pettigrew 2003; Baron et al. 2007; Ng et al. 2010). Complementing these neurobiological investigations are behavioral studies demonstrating that birds also respond behaviorally to these pattern attributes. For example, in nearly 30 different avian taxa, behavioral studies have shown that birds respond to changes in the spatial frequency and contrast of visual stimuli, and this sensitivity varies greatly across species (Caves et al. 2018). Furthermore, chicks (*Gallus gallus*) and pigeons (*C. livia*) can be trained to respond differentially to patterns with different orientations (Blough 1985; Blough and Franklin 1985; Jones and Osorio 2004). Studies in other animal taxa, such as mammals, also demonstrate sensitivity to spatial frequency, orientation, and contrast (Van Hooser 2007), suggesting that these visual features play a fundamental role in orienting, navigation, object recognition, and other basic visual/cognitive tasks.

We acknowledge that the metrics we derive from the three-dimensional pattern space (pattern diversity and pattern uniqueness) have not been tested for visual salience in animals in the way that spatial frequency, orientation, and contrast have been. However, we believe that these measures are worthwhile aspects of patterning to analyze in an evolutionary framework, as they can potentially reveal insights about constraints and/or nonsignaling functions of pattern. We also note that these derived pattern measures are dependent on the metrics chosen to serve as dimensions of the pattern space, which will depend on the nature of the patterns being analyzed and the research questions being investigated. For example, removing the contrast dimension yields different results for pattern diversity, emphasizing qualitative differences in patterning (i.e., streaks vs. barring). See figure S4 for a comparison of three-dimensional and two-dimensional pattern diversity plotted on the phylogenetic tree. Alternatively, adding luminance (brightness) as a dimension could provide additional utility for testing hypotheses about crypsis or signaling, as it would separate, for example, solid-plumaged species with all white plumage versus all black plumage.

Furthermore, we acknowledge that by modeling pattern traits as continuous traits, we are assuming that these traits evolve incrementally, which may be an imperfect assump-

tion. For example, there is some evidence from other bird taxa that barring patterns may be a plumage “syndrome” controlled by a suite of genes that can easily be turned on or off (Smith and Nordskog 1963; Hollander 1968; Crawford 1990; Gluckman and Mundy 2016). However, it is also clear from our study that spatial frequency and contrast of barring patterns vary across a more or less continuous spectrum (fig. 3). Finally, treating pattern traits categorically requires subjective decision-making by human viewers, which is something we wanted to avoid in our study. There are some species (e.g., members of the genus *Sphyrapicus*) with patterning that is somewhere in between spots, streaks, and mottling, making these patterns difficult to categorize qualitatively.

Pattern Variation in Pattern Space

The distribution of the melanerpine woodpecker plumage patterns in morphospace (figs. 3, 5) indicates influences of phylogenetic and mechanistic constraint, as well as functional adaptation, on pattern evolution. Species occupying similar areas of pattern space tend to be closely related, such as the barred-back “Centurus” species (in magenta, figs. 3, 5D) and the mottled *Sphyrapicus* sapsuckers (in dark blue, figs. 3, 5D), suggesting that plumage pattern exhibits some degree of phylogenetic constraint. However, our ancestral state estimates imply multiple independent origins for some traits, such as dorsal barring, across the melanerpine tree (e.g., in gray-breasted woodpecker [*M. hypopolius*], Hispaniolan woodpecker [*M. striatus*], and black-cheeked woodpecker [*M. pucherani*]; fig. 5D). Dorsal barring may therefore be an evolutionarily labile trait that can evolve relatively quickly. Support for this idea comes from work in waterfowl (Anseriformes) and game birds (Galliformes), showing that barring can evolve directly from uniform plumage without requiring a transitional pattern phase (Gluckman and Mundy 2016). In addition, genetic studies have shown that a single mutation can lead to the appearance of barring in Muscovy ducks (*Cairina moschata*; Hollander 1968) and uniformly colored chickens (*Gallus domesticus*; Smith and Nordskog 1963; Crawford 1990). Furthermore, unlike its male counterpart, the female Williamson’s sapsucker (*Sphyrapicus thyroideus*) displays extensive dorsal barring, resulting in an uncanny resemblance to species in the “Centurus” subclade and providing further evidence for high lability in the dorsal barring trait. Females of the closest relatives of *S. thyroideus*, yellow-bellied sapsucker (*S. varius*) and red-breasted sapsucker (*S. ruber*), lack dorsal barring, suggesting that barring is more likely to have appeared as a novel trait in female *S. thyroideus* instead of being lost in the male. While we did not analyze female plumage in the current study, future work should

explore how female melanerpine woodpeckers evolved to occupy the plumage pattern morphospace relative to males.

Plotting melanerpine subclades in pattern space reveals significant overlap among subclades (fig. 5A–5C) owing to common plumage patterns found across the melanerpine tree. For example, dorsal barring appears in nearly every subclade, as does solid chest plumage (fig. 5D). However, we do find differences in the extent of species overlap within subclades: species in the “typical Melanerpes” subclade (fig. 5D) display the most variation in plumage pattern (fig. 5I, 5J) as measured by both convex hull overlap and Euclidean distances, and they possess different rates of pattern evolution in terms of contrast (higher rate of phenotypic evolution) and horizontal pattern orientation (lower rate of phenotypic evolution; fig. 6B). This group also contains the three most unique melanerpine species as measured by our pattern uniqueness metric: white woodpecker (*M. candidus*), acorn woodpecker (*M. formicivorus*), and Lewis’s woodpecker (*M. lewis*; fig. 5D). Despite its nickname, the “typical Melanerpes” subclade includes species with atypical behaviors among melanerpines. For example, white-fronted woodpecker (*M. cactorum*) and acorn woodpecker (*M. formicivorus*) are both cooperative breeders, and the latter builds enormous acorn granaries in trees (Winkler et al. 2013; Winkler and Christie 2015). Red-headed woodpecker (*M. erythrocephalus*) and Lewis’s woodpecker (*M. lewis*) rely heavily on fly catching for food; the former is the only woodpecker species known to conceal its food caches with bark, while the latter is partially migratory, an unusual behavior for woodpeckers in general (Frei et al. 2020; Vierling et al. 2020). White woodpecker (*M. candidus*) is different in that it primarily consumes fruit (Winkler et al. 2020). These atypical behaviors may have led to changes in rates of pattern evolution via mechanisms such as signaling needs in a cooperative breeding system or changes in predation pressure due to evolutionary innovations in foraging.

Ecological Correlates of Plumage Patterning

Our finding that smaller melanerpine species are more likely than larger species to have horizontally oriented patterning on the face (table S4) suggests that crypsis may be a selective pressure on woodpecker plumage patterns. Because smaller-bodied birds are typically at a greater risk of predation (Götmark and Post 1996) as well as aggression (Leighton et al. 2018) from larger-bodied species, smaller species may be under greater selective pressure than larger species to avoid being detected. Most of the horizontally oriented patterning that we observe in the melanerpines consists of either an elongated dark marking that completely encompasses the eye or a marking whose border intersects the eye (see fig. 1 for views of the face). These types of markings, often called “eye stripes,” have been shown to

serve a predator-avoidance function in fish (Kjernsmo et al. 2016). In birds, eye stripes have been shown to obscure detection of the eye in human vision experiments, with the effect being strongest when the eye is on the edge of the marking (Gavish and Gavish 1981). Given these findings, eye stripe prevalence in smaller melanerpine species may be an adaptation to avoid detection by predators and/or larger competitors. Alternatively, the relationship between eye stripe and body size may be driven by developmental constraints rather than selection, since surface area and shape influence pattern development (Murray 1981; Murray et al. 1990; Price and Pavelka 1996; Riegner 2008). These studies predict the opposite of what we found, however: smaller surface areas can support less patterning than larger surface areas, and therefore the smallest animals and/or smallest body parts tend to be solid instead of patterned (Murray 1981, 1988; Murray et al. 1990; Price 2006; Riegner 2008). In our study, larger species tend to have solid faces, and therefore our findings are more in line with an adaptive function of crypsis.

We also note that the PGLS multiple linear regression model with chest contrast as the outcome variable was approaching significance ($R^2_{\text{pred}} = 0.59$, $F_{23,16} = 3.73$, $P = .07$; table S4); within this model, there was a significant positive correlation between chest contrast and habitat openness ($\beta = 1.21$, $SE = 0.34$, $t = 3.50$, $P = .003$; table S5): melanerpine species living in more open habitats display more contrast within their chest plumage than those living in more closed habitats. This trend is in line with a broad-scale study of woodpecker color patterns that found that boldly patterned woodpeckers are more commonly found in open habitats (Miller et al. 2019). Future work is needed to determine the evolutionary forces (e.g., signaling, crypsis) that may drive the relationship between light environment and plumage contrast.

Developmental and Physiological Constraints on Plumage Pattern Evolution

Physiological constraints likely play a role in shaping the melanerpine plumage pattern morphospace. For example, the area of the space corresponding to horizontally oriented patterns with low spatial frequencies (i.e., wide barring) is mostly unoccupied (figs. 3–5). Plumage patterns across the body are created by overlapping feathers, which themselves display within-feather patterning; the within-feather patterning is produced by the deposition of melanosomes into the feather barbs and barbules as the feather grows (Prum and Williamson 2002). The interplay of these processes constrains the types of patterns that can be created (Prum and Williamson 2002); wide bars may thus be difficult to achieve. Alternatively, a particular type of pattern may be physiologically possible but may not occur in the

melanerpine woodpeckers owing to phylogenetic history: perhaps the crucial genes or regulatory factors for some patterns were lost or were never present in an ancestor of the group. Circular spots, for example, would hypothetically occupy the area of pattern space corresponding to high spatial frequency, high contrast, and equal contribution of horizontal and vertical pattern information (i.e., an orientation value near zero); in the melanerpine woodpeckers, this area of pattern space is sparsely populated (figs. 3–5). Spots are physiologically possible to produce, as they exist in other woodpeckers, such as northern flicker (*Colaptes auratus*), as well as in many other birds. However, evidence from a study on waterfowl (Anseriformes) and game birds (Galliformes) suggests that spots are difficult to evolve in that they require a transitional pattern, such as bars; in other words, spots cannot evolve directly from uniform plumage (Gluckman and Mundy 2016). If this is indeed the case in woodpeckers, circular spots could theoretically evolve from barred plumage, but we do not observe this progression.

Phenotypic integration, also known as morphological integration or trait covariation, of plumage patterns (i.e., displaying the same patterns in different patches of the plumage) could also indicate physiological and/or developmental constraints in pattern development (Cheverud 1996). In our analysis, we did not find evidence for phenotypic integration of pattern traits across the patches of interest we analyzed (the upper dorsum, chest, and face), except that the face and chest covaried in terms of spatial frequency (table S7). This suggests that plumage patterns across the body evolve mostly independently, possibly responding to different selective pressures.

Application to the Study of Diverse Animal Coloration Patterns

In this study we used a pattern space to describe the evolution of plumage patterns in the melanerpine woodpeckers, but our methods can be applied broadly to the study of integument patterns in any animal taxa. Just as the concept of a color space in recent decades led to an explosion of comparative studies and deepened our understanding of color evolution across the tree of life (Renoult et al. 2015), pattern morphospace analyses have the potential to do the same for the evolution of animal patterns (Stoddard and Osorio 2019; Mason and Bowie 2020). The long-standing question of how natural selection and constraint interact to create stunning diversity as well as common motifs in animal patterns continues to captivate evolutionary biologists and has resulted in a number of comparative studies across a diverse range of animal taxa, including snakes (Allen et al. 2013; Davis Rabosky et al. 2016), primates (Allen et al. 2014; Allen and Higham 2015), carnivores (Ortolani 1999; Allen

et al. 2011), artiodactyls (Stoner 2003), rodents (Ancillotto and Mori 2017), lagomorphs (Stoner et al. 2003), geckos (Allen et al. 2019), fish (Endler 1982; Seehausen et al. 1999), butterflies (Jiggins et al. 2006; Oliver et al. 2009), and birds (Gomez and Théry 2004; Weibel and Moore 2005; Gluckman and Cardoso 2010; Marshall and Gluckman 2015; Maia et al. 2016; Somveille et al. 2016; Miller et al. 2019; Mason and Bowie 2020; Beco et al. 2021). In these and other systems there are many outstanding lines of inquiry for which pattern morphospace analyses—like those we have applied here—could provide new insights about pattern evolution across the animal kingdom.

Acknowledgments

We thank Nicholas DeWind for assistance with coding the two-dimensional fast Fourier transformation analysis, Joseph Kawalec for help with image processing, Derya Akkaynak for helpful discussions, Audrey Miller for help with photography, Klara Nordén and Jarome Ali for helpful comments on the manuscript, Nate Rice at the Academy of Natural Sciences of Drexel University and Paul Sweet at the American Museum of Natural History for assistance with museum specimens, and the specimen collectors, preparators, and their assistants, many of whom go unnamed and unrecognized but without whom this work would not have been possible. We also thank the Macaulay Library at the Cornell Lab of Ornithology for media resources. For funding support, we thank Princeton University (M.L.C. and M.C.S.) and a Packard Fellowship for Science and Engineering (M.C.S.).

Statement of Authorship

M.L.C. and M.C.S. conceived the project; M.L.C. collected and analyzed the data; M.L.C. wrote the initial draft of the manuscript; and M.L.C. and M.C.S. wrote subsequent versions of the manuscript.

Data and Code Availability

All data and code are available in the Dryad Digital Repository (<https://doi.org/10.5061/dryad.2rbnzs7qq>; Carlson and Stoddard 2023).

Literature Cited

- Adams, D. C., M. L. Collyer, A. Kaliontzopoulou, and E. K. Baken. 2021. geomorph: software for geometric morphometric analyses. R package version 4.0. <https://CRAN.R-project.org/package=geomorph>.
- Allen, W. L., R. Baddeley, N. E. Scott-Samuel, and I. C. Cuthill. 2013. The evolution and function of pattern diversity in snakes. *Behavioral Ecology* 24:1237–1250.

- Allen, W. L., I. C. Cuthill, N. E. Scott-Samuel, and R. Baddeley. 2011. Why the leopard got its spots: relating pattern development to ecology in felids. *Proceedings of the Royal Society B* 278:1373–1380.
- Allen, W. L., and J. P. Higham. 2015. Assessing the potential information content of multicomponent visual signals: a machine learning approach. *Proceedings of the Royal Society B* 282:20142284.
- Allen, W. L., N. Moreno, T. Gamble, and Y. Chiari. 2019. Ecological, behavioral and phylogenetic influences on the evolution of dorsal color pattern in geckos. *Evolution* 74:1033–1047.
- Allen, W. L., M. Stevens, and J. P. Higham. 2014. Character displacement of *Cercopithecini* primate visual signals. *Nature Communications* 5:4266.
- Ancillotto, L., and E. Mori. 2017. Adaptive significance of coat colouration and patterns of Sciuromorpha (Rodentia). *Ethology Ecology and Evolution* 29:241–254.
- Baken, E. K., M. L. Collyer, A. Kaliontzopoulou, and D. C. Adams. 2021. geomorph v4.0 and gmShiny: enhanced analytics and a new graphical interface for a comprehensive morphometric experience. *Methods in Ecology and Evolution* 12:2355–2363.
- Ballard, D., and C. M. Brown. 1982. *Computer vision*. Prentice Hall, Englewood Cliffs, NJ.
- Barbosa, A., L. M. Mäthger, K. C. Buresch, J. Kelly, C. Chubb, C.-C. Chiao, and R. T. Hanlon. 2008. Cuttlefish camouflage: the effects of substrate contrast and size in evoking uniform, mottle or disruptive body patterns. *Vision Research* 48:1242–1253.
- Baron, J., L. Pinto, M. O. Dias, B. Lima, and S. Neuenschwander. 2007. Directional responses of visual wulst neurones to grating and plaid patterns in the awake owl. *European Journal of Neuroscience* 26:1950–1968.
- Beco, R., L. F. Silveira, E. P. Derryberry, and G. A. Bravo. 2021. Ecology and behavior predict an evolutionary trade-off between song complexity and elaborate plumages in antwrens (Aves, Thamnophilidae). *Evolution* 75:2388–2410.
- Belleghem, S. M. V., R. Papa, H. Ortiz-Zuazaga, F. Hendrickx, C. D. Jiggins, W. O. McMillan, and B. A. Counterman. 2018. patternize: an R package for quantifying colour pattern variation. *Methods in Ecology and Evolution* 9:390–398.
- Benjamini, Y., and Y. Hochberg. 1995. Controlling the false discovery rate: a practical and powerful approach to multiple testing. *Journal of the Royal Statistical Society B* 57:289–300.
- Blough, D. S. 1985. Discrimination of letters and random dot patterns by pigeons and humans. *Journal of Experimental Psychology* 11:261–280.
- Blough, D. S., and J. J. Franklin. 1985. Pigeon discrimination of letters and other forms in texture displays. *Perception and Psychophysics* 38:523–532.
- Carlson, M. L., and M. C. Stoddard. 2023. Data from: Evolution of plumage patterns in a pattern morphospace: a phylogenetic analysis of melanerpine woodpeckers. *American Naturalist*, Dryad Digital Repository, <https://doi.org/10.5061/dryad.2rbnzs7qq>.
- Caves, E. M., N. C. Brandley, and S. Johnsen. 2018. Visual acuity and the evolution of signals. *Trends in Ecology and Evolution* 33:358–372.
- Cheverud, J. M. 1996. Developmental integration and the evolution of pleiotropy. *American Zoologist* 36:44–50.
- Chiao, C.-C., C. Chubb, K. Buresch, L. Siemann, and R. T. Hanlon. 2009. The scaling effects of substrate texture on camouflage patterning in cuttlefish. *Vision Research* 49:1647–1656.
- Crawford, R. D. 1990. *Poultry breeding and genetics*. Developments in Animal and Veterinary Science. Elsevier, Amsterdam.
- Davis Rabosky, A. R., C. L. Cox, D. L. Rabosky, P. O. Title, I. A. Holmes, A. Feldman, and J. A. McGuire. 2016. Coral snakes predict the evolution of mimicry across New World snakes. *Nature Communications* 7:11484.
- Dunning, J. B. 2008. *CRC handbook of avian body masses*. 2nd ed. CRC, Boca Raton, FL.
- Endler, J. A. 1982. Convergent and divergent effects of natural selection on color patterns in two fish faunas. *Evolution* 36:178–188.
- . 1983. Natural and sexual selection on color patterns in poeciliid fishes. *Environmental Biology of Fishes* 9:173–190.
- . 2012. A framework for analysing colour pattern geometry: adjacent colours. *Biological Journal of the Linnean Society* 107:233–253.
- Endler, J. A., and P. W. Mielke. 2005. Comparing entire colour patterns as birds see them. *Biological Journal of the Linnean Society* 86:405–431.
- Felsenstein, J. 1973. Maximum-likelihood estimation of evolutionary trees from continuous characters. *American Journal of Human Genetics* 25:471–492.
- . 1985. Phylogenies and the comparative method. *American Naturalist* 125:1–15.
- Frei, B., K. G. Smith, J. H. Withgott, P. G. Rodewald, P. Pyle, and M. A. Patten. 2020. Red-headed woodpecker (*Melanerpes erythrocephalus*), version 1.0. In P. G. Rodewald, ed. *Birds of the world*. Cornell Lab of Ornithology, Ithaca, NY.
- Gaffney, M. F., and W. Hodos. 2003. The visual acuity and refractive state of the American kestrel (*Falco sparverius*). *Vision Research* 43:2053–2059.
- Galván, I., J. García-Campa, and J. J. Negro. 2017. Complex plumage patterns can be produced only with the contribution of melanins. *Physiological and Biochemical Zoology* 90:600–604.
- Gavish, L., and B. Gavish. 1981. Patterns that conceal a bird's eye. *Zeitschrift für Tierpsychologie* 56:193–204.
- Ghim, M. M., and W. Hodos. 2006. Spatial contrast sensitivity of birds. *Journal of Comparative Physiology A* 192:523–534.
- Gluckman, T.-L., and G. C. Cardoso. 2010. The dual function of barred plumage in birds: camouflage and communication. *Journal of Evolutionary Biology* 23:2501–2506.
- Gluckman, T.-L., and N. I. Mundy. 2016. Evolutionary pathways to convergence in plumage patterns. *BMC Evolutionary Biology* 16:172.
- Godfrey, D., J. N. Lythgoe, and D. A. Rumball. 1987. Zebra stripes and tiger stripes: the spatial frequency distribution of the pattern compared to that of the background is significant in display and crypsis. *Biological Journal of the Linnean Society* 32:427–433.
- Gomez, D., and M. Théry. 2004. Influence of ambient light on the evolution of colour signals: comparative analysis of a Neotropical rainforest bird community. *Ecology Letters* 7:279–284.
- Götmark, F., and P. Post. 1996. Prey selection by sparrowhawks, *Accipiter nisus*: relative predation risk for breeding passerine birds in relation to their size, ecology and behaviour. *Philosophical Transactions of the Royal Society B* 351:1559–1577.
- Harmon, L. J., J. T. Weir, C. D. Brock, R. E. Glor, and W. Challenger. 2008. GEIGER: investigating evolutionary radiations. *Bioinformatics* 24:129–131.
- Hollander, W. F. 1968. Brown-rippled, a recessive mutant in the muscovy duck. *Journal of Heredity* 59:309–311.
- Hubel, D. H., and T. N. Wiesel. 1959. Receptive fields of single neurones in the cat's striate cortex. *Journal of Physiology* 148:574–591.
- . 1968. Receptive fields and functional architecture of monkey striate cortex. *Journal of Physiology* 195:215–243.

- Inaba, M., and C.-M. Chuong. 2020. Avian pigment pattern formation: developmental control of macro- (across the body) and micro- (within a feather) level of pigment patterns. *Frontiers in Cell and Developmental Biology* 8:620.
- Jiggins, C. D., R. Mallarino, K. R. Willmott, and E. Bermingham. 2006. The phylogenetic pattern of speciation and wing pattern change in Neotropical *Ithomia* butterflies (Lepidoptera: Nymphalidae). *Evolution* 60:1454–1466.
- Jones, C. D., and D. Osorio. 2004. Discrimination of oriented visual textures by poultry chicks. *Vision Research* 44:83–89.
- Kang, C., M. Stevens, J. Moon, S.-I. Lee, and P. G. Jablonski. 2015. Camouflage through behavior in moths: the role of background matching and disruptive coloration. *Behavioral Ecology* 26:45–54.
- Kemp, D. J., M. E. Herberstein, L. J. Fleishman, J. A. Endler, A. T. D. Bennett, A. G. Dyer, N. S. Hart, J. Marshall, and M. J. Whiting. 2015. An integrative framework for the appraisal of coloration in nature. *American Naturalist* 185:705–724.
- Kjernsmo, K., M. Grönholm, and S. Merilaita. 2016. Adaptive constellations of protective marks: eyespots, eye stripes and diversion of attacks by fish. *Animal Behaviour* 111:189–195.
- Lee, J.-Y., L. A. Holden, and M. B. A. Djamgoz. 1997. Effects of ageing on spatial aspects of the pattern electroretinogram in male and female quail. *Vision Research* 37:505–514.
- Leighton, G. M., A. C. Lees, and E. T. Miller. 2018. The hairy-downy game revisited: an empirical test of the interspecific social dominance mimicry hypothesis. *Animal Behaviour* 137:141–148.
- Liu, G. B., and J. D. Pettigrew. 2003. Orientation mosaic in barn owl's visual Wulst revealed by optical imaging: comparison with cat and monkey striate and extra-striate areas. *Brain Research* 961:153–158.
- Maia, R., D. R. Rubenstein, and M. D. Shawkey. 2016. Selection, constraint, and the evolution of coloration in African starlings. *Evolution* 70:1064–1079.
- Marcondes, R. S., and R. T. Brumfield. 2020. A simple index to quantify and compare the magnitude of intraspecific geographic plumage colour variation in typical antbirds (Aves: Passeriformes: Thamnophilidae). *Biological Journal of the Linnean Society* 130:239–246.
- Marques, C. I. J., H. R. Batalha, and G. C. Cardoso. 2016. Signaling with a cryptic trait: the regularity of barred plumage in common waxbills. *Royal Society Open Science* 3:160195.
- Marshall, K. L. A., and T.-L. Gluckman. 2015. The evolution of pattern camouflage strategies in waterfowl and game birds. *Ecology and Evolution* 5:1981–1991.
- Mason, N. A., and R. C. K. Bowie. 2020. Plumage patterns: ecological functions, evolutionary origins, and advances in quantification. *Auk* 137:ukaa060.
- Mason, N. A., E. A. Riddell, F. Romero, C. Cicero, and R. C. K. Bowie. 2021. Plumage balances camouflage and thermoregulation in horned larks (*Eremophila alpestris*). *bioRxiv*, <https://doi.org/10.1101/2021.07.15.452373>.
- Mazer, J. A., W. E. Vinje, J. McDermott, P. H. Schiller, and J. L. Gallant. 2002. Spatial frequency and orientation tuning dynamics in area V1. *Proceedings of the National Academy of Sciences of the USA* 99:1645–1650.
- Medina, L., and A. Reiner. 2000. Do birds possess homologues of mammalian primary visual, somatosensory and motor cortices? *Trends in Neurosciences* 23:1–12.
- Miller, E. T., G. M. Leighton, B. G. Freeman, A. C. Lees, and R. A. Ligon. 2019. Ecological and geographical overlap drive plumage evolution and mimicry in woodpeckers. *Nature Communications* 10:1602.
- Murray, J. D. 1981. A pre-pattern formation mechanism for animal coat markings. *Journal of Theoretical Biology* 88:161–199.
- . 1988. How the leopard gets its spots. *Scientific American* 258:80–87.
- Murray, J. D., D. C. Deeming, and M. W. J. Ferguson. 1990. Size-dependent pigmentation-pattern formation in embryos of *Alligator mississippiensis*: time of initiation of pattern generation mechanism. *Proceedings of the Royal Society B* 239:279–293.
- Navarro-Sigüenza, A. G., H. Vázquez-Miranda, G. Hernández-Alonso, E. A. García-Trejo, and L. A. Sánchez-González. 2017. Complex biogeographic scenarios revealed in the diversification of the largest woodpecker radiation in the New World. *Molecular Phylogenetics and Evolution* 112:53–67.
- Ng, B. S. W., A. Grabska-Barwińska, O. Güntürkün, and D. Jancke. 2010. Dominant vertical orientation processing without clustered maps: early visual brain dynamics imaged with voltage-sensitive dye in the pigeon visual Wulst. *Journal of Neuroscience* 30:6713–6725.
- Nieder, A., and H. Wagner. 2001. Encoding of both vertical and horizontal disparity in random-dot stereograms by Wulst neurons of awake barn owls. *Visual Neuroscience* 18:541–547.
- Nokelainen, O., N. E. Scott-Samuel, Y. Nie, F. Wei, and T. Caro. 2021. The giant panda is cryptic. *Scientific Reports* 11:21287.
- Oliver, J. C., K. A. Robertson, and A. Monteiro. 2009. Accommodating natural and sexual selection in butterfly wing pattern evolution. *Proceedings of the Royal Society B* 276:2369–2375.
- Ortolani, A. 1999. Spots, stripes, tail tips and dark eyes: predicting the function of carnivore colour patterns using the comparative method. *Biological Journal of the Linnean Society* 67:433–476.
- Paradis, E., and K. Schliep. 2019. ape 5.0: an environment for modern phylogenetics and evolutionary analyses in R. *Bioinformatics* 35:526–528.
- Pettigrew, J. D., and M. Konishi. 1976. Neurons selective for orientation and binocular disparity in the visual Wulst of the barn owl (*Tyto alba*). *Science* 193:675–678.
- Porciatti, V., G. Fontanesi, and P. Bagnoli. 1989. The electroretinogram of the little owl (*Athene noctua*). *Vision Research* 29:1693–1698.
- Price, T. D. 2006. Phenotypic plasticity, sexual selection and the evolution of colour patterns. *Journal of Experimental Biology* 209:2368–2376.
- Price, T., and M. Pavelka. 1996. Evolution of a colour pattern: history, development, and selection. *Journal of Evolutionary Biology* 9:451–470.
- Prum, R. O., and S. Williamson. 2002. Reaction-diffusion models of within-feather pigmentation patterning. *Proceedings of the Royal Society B* 269:781–792.
- Renoult, J. P., A. Kelber, and H. M. Schaefer. 2015. Colour spaces in ecology and evolutionary biology. *Biological Reviews* 92:292–315.
- Revell, L. J. 2012. phytools: an R package for phylogenetic comparative biology (and other things). *Methods in Ecology and Evolution* 3:217–223.
- Riegner, M. F. 2008. Parallel evolution of plumage pattern and coloration in birds: implications for defining avian morphospace. *Condor* 110:599–614.
- Rosenthal, G. G. 2007. Spatiotemporal dimensions of visual signals in animal communication. *Annual Review of Ecology, Evolution, and Systematics* 38:155–178.
- Ruxton, G. D., T. N. Sherratt, and M. P. Speed. 2004. *Avoiding attack: the evolutionary ecology of crypsis, warning signals and mimicry*. Oxford University Press, Oxford.

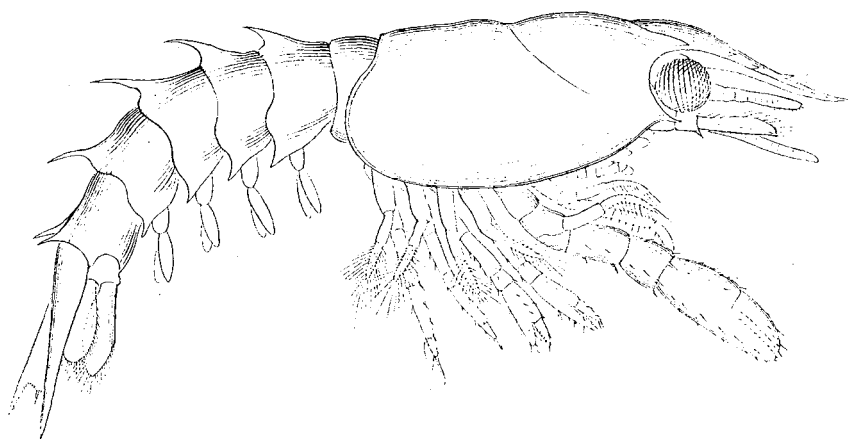
- Schluter, D., T. Price, A. Ø. Mooers, and D. Ludwig. 1997. Likelihood of ancestor states in adaptive radiation. *Evolution* 51:1699–1711.
- Seehausen, M., and J. J. M. V. Alphen. 1999. Evolution of colour patterns in East African cichlid fish. *Journal of Evolutionary Biology* 12:514–534.
- Shakya, S. B., J. Fuchs, J.-M. Pons, and F. H. Sheldon. 2017. Tapping the woodpecker tree for evolutionary insight. *Molecular Phylogenetics and Evolution* 116:182–191.
- Short, L. 1982. *Woodpeckers of the world*. Delaware Museum of Natural History, Greenville, DE.
- Smith, L. T., and A. W. Nordskog. 1963. Studies on dominance and pleiotropy using segregating inbred lines of fowl. *Genetics* 48:1141–1152.
- Somveille, M., K. L. A. Marshall, and T.-L. Gluckman. 2016. A global analysis of bird plumage patterns reveals no association between habitat and camouflage. *PeerJ* 4:e2658.
- Stevens, M., and I. C. Cuthill. 2006. Disruptive coloration, crypsis and edge detection in early visual processing. *Proceedings of the Royal Society B* 273:2141–2147.
- Stevens, M., A. E. Lown, and L. E. Wood. 2014. Camouflage and individual variation in shore crabs (*Carcinus maenas*) from different habitats. *PLoS ONE* 9:e115586.
- Stevens, M., C. A. Párraga, I. C. Cuthill, J. C. Partridge, and T. S. Troscianko. 2007. Using digital photography to study animal coloration. *Biological Journal of the Linnean Society* 90:211–237.
- Stevens, M., J. Troscianko, J. K. Wilson-Aggarwal, and C. N. Spottiswoode. 2017. Improvement of individual camouflage through background choice in ground-nesting birds. *Nature Ecology and Evolution* 1:1325–1333.
- Stoddard, M. C., B. G. Hogan, M. Stevens, and C. N. Spottiswoode. 2019. Higher-level pattern features provide additional information to birds when recognizing and rejecting parasitic eggs. *Philosophical Transactions of the Royal Society B* 374:20180197.
- Stoddard, M. C., R. M. Kilner, and C. Town. 2014. Pattern recognition algorithm reveals how birds evolve individual egg pattern signatures. *Nature Communications* 5:4117.
- Stoddard, M. C., K. Kupán, H. N. Eyster, W. Rojas-Abreu, M. Cruz-López, M. A. Serrano-Meneses, and C. Küpper. 2016. Camouflage and clutch survival in plovers and terns. *Scientific Reports* 6:32059.
- Stoddard, M. C., and D. Osorio. 2019. Animal coloration patterns: linking spatial vision to quantitative analysis. *American Naturalist* 193:164–186.
- Stoddard, M. C., and R. O. Prum. 2008. Evolution of avian plumage color in a tetrahedral color space: a phylogenetic analysis of New World buntings. *American Naturalist* 171:755–776.
- Stoddard, M. C., and M. Stevens. 2010. Pattern mimicry of host eggs by the common cuckoo, as seen through a bird's eye. *Proceedings of the Royal Society B* 277:1387–1393.
- Stoner, C. J. 2003. Ecological and behavioral correlates of coloration in artiodactyls: systematic analyses of conventional hypotheses. *Behavioral Ecology* 14:823–840.
- Stoner, C. J., O. R. P. Bininda-Emonds, and T. Caro. 2003. The adaptive significance of coloration in lagomorphs. *Biological Journal of the Linnean Society* 79:309–328.
- Troscianko, J., O. Nokelainen, J. Skelhorn, and M. Stevens. 2021. Variable crab camouflage patterns defeat search image formation. *Communications Biology* 4:287.
- Troscianko, J., J. Skelhorn, and M. Stevens. 2017. Quantifying camouflage: how to predict detectability from appearance. *BMC Evolutionary Biology* 17:7.
- Troscianko, J., and M. Stevens. 2015. Image calibration and analysis toolbox: a free software suite for objectively measuring reflectance, colour and pattern. *Methods in Ecology and Evolution* 6:1320–1331.
- van den Berg, C. P., J. Troscianko, J. A. Endler, N. J. Marshall, and K. L. Cheney. 2020. Quantitative colour pattern analysis (QCPA): a comprehensive framework for the analysis of colour patterns in nature. *Methods in Ecology and Evolution* 11:316–332.
- Van Hooser, S. D. 2007. Similarity and diversity in visual cortex: is there a unifying theory of cortical computation? *Neuroscientist* 13:639–656.
- Vierling, K. T., V. A. Saab, and B. W. Tobalske. 2020. Lewis's woodpecker (*Melanerpes lewis*), version 1.0. In A. F. Poole, ed. *Birds of the world*. Cornell Lab of Ornithology, Ithaca, NY.
- Weibel, A. C., and W. S. Moore. 2005. Plumage convergence in *Picoides* woodpeckers based on a molecular phylogeny, with emphasis on convergence in downy and hairy woodpeckers. *Condor* 107:797.
- Westmoreland, D., and R. A. Kiltie. 1996. Egg crypsis and clutch survival in three species of blackbirds (Icteridae). *Biological Journal of the Linnean Society* 58:159–172.
- Winkler, H., and D. A. Christie. 2013. Gila woodpecker (*Melanerpes uropygialis*). In J. del Hoyo, A. Elliott, J. Sargatal, D. A. Christie, and E. de Juana, eds. *Handbook of birds of the world alive*. Lynx, Barcelona.
- . 2015. Acorn woodpecker (*Melanerpes formicivorus*). In J. del Hoyo, A. Elliott, J. Sargatal, D. A. Christie, and E. de Juana, eds. *Handbook of birds of the world alive*. Lynx, Barcelona.
- Winkler, H., D. A. Christie, and A. Bonan. 2013. White-fronted woodpecker (*Melanerpes cactorum*). In J. del Hoyo, A. Elliott, J. Sargatal, D. A. Christie, and E. de Juana, eds. *Handbook of birds of the world alive*. Lynx, Barcelona.
- Winkler, H., D. A. Christie, and E. de Juana. 2018. Guadeloupe woodpecker (*Melanerpes herminieri*). In J. del Hoyo, A. Elliott, J. Sargatal, D. A. Christie, and E. de Juana, eds. *Handbook of birds of the world alive*. Lynx, Barcelona.
- Winkler, H., D. A. Christie, and G. M. Kirwan. 2020. White woodpecker (*Melanerpes candidus*), version 1.0. In J. del Hoyo, A. Elliott, J. Sargatal, D. A. Christie, and E. de Juana, eds. *Birds of the world*. Cornell Lab of Ornithology, Ithaca, NY.
- Zhou, W., L. Yu, B. Z. W. Kwek, G. Jin, H. Zeng, and D. Li. 2021. Sexual selection on jumping spider color pattern: investigation with a new quantitative approach. *Behavioral Ecology* 32:695–706.

References Cited Only in the Online Enhancements

- Adams, D. C. 2014. Quantifying and comparing phylogenetic evolutionary rates for shape and other high-dimensional phenotypic data. *Systematic Biology* 63:166–177.
- Allen, E. J., P. C. Burton, J. Mesik, C. A. Olman, and A. J. Oxenham. 2019. Cortical correlates of attention to auditory features. *Journal of Neuroscience* 39:3292–3300.
- Anantharaman, J. N., A. K. Krishnamurthy, and L. L. Feth. 1993. Intensity-weighted average of instantaneous frequency as a model for frequency discrimination. *Journal of the Acoustical Society of America* 94:723–729.
- Blomberg, S. P., T. Garland, and A. R. Ives. 2003. Testing for phylogenetic signal in comparative data: behavioral traits are more labile. *Evolution* 57:717.

- Bovik, A. C. 2009. *The essential guide to image processing*. Elsevier, San Diego.
- Caves, E. M., and S. Johnsen. 2017. AcuityView: an R package for portraying the effects of visual acuity on scenes observed by an animal. *Methods in Ecology and Evolution* 9:793–797.
- Coffin, D. 2008. DCRAW: decoding raw digital photos in Linux. <https://www.dechifro.org/dcraw/>.
- Denton, J. S. S., and D. C. Adams. 2015. A new phylogenetic test for comparing multiple high-dimensional evolutionary rates suggests interplay of evolutionary rates and modularity in lanternfishes (Myctophiformes; Myctophidae). *Evolution* 69:2425–2440.
- Field, D. J. 1987. Relations between the statistics of natural images and the response properties of cortical cells. *Journal of the Optical Society of America A* 4:2379.
- Fox, J., and S. Weisberg. 2019. *An R companion to applied regression*. 3rd ed. Sage, Thousand Oaks, CA.
- Grey, J. M., and J. W. Gordon. 1978. Perceptual effects of spectral modifications on musical timbres. *Journal of the Acoustical Society of America* 63:1493–1500.
- Gruson, H. 2020. Estimation of colour volumes as concave hyper-volumes using α -shapes. *Methods in Ecology and Evolution* 11:955–963.
- Harmon, L. 2019. *Phylogenetic comparative methods*. Open Textbook Library, Minneapolis.
- Hart, N. S. 2002. Vision in the peafowl (*Aves: Pavo cristatus*). *Journal of Experimental Biology* 205:3925.
- Ives, A. R. 2019. R^2 s for correlated data: phylogenetic models, LMMs, and GLMMs. *Systematic Biology* 68:234–251.
- Le, P. N., E. Ambikairajah, J. Epps, V. Sethu, and E. H. C. Choi. 2011. Investigation of spectral centroid features for cognitive load classification. *Speech Communication* 53:540–551.
- Mahmood, F., M. Toots, L.-G. Öfverstedt, and U. Skoglund. 2015. 2D discrete Fourier transform with simultaneous edge artifact removal for real-time applications. Pages 236–239 in 2015 International Conference on Field Programmable Technology (FPT). IEEE, Piscataway, NJ.
- Menard, S. 1995. *Applied logistic regression analysis*. Sage University Series on Quantitative Applications in the Social Sciences. Sage, Thousand Oaks, CA.
- Ödeen, A., and O. Håstad. 2003. Complex distribution of avian color vision systems revealed by sequencing the SWS1 opsin from total DNA. *Molecular Biology and Evolution* 20:855–861.
- Pinheiro, J. C., D. Bates, S. DebRoy, D. Sarkar, and R Core Team. 2019. nlme: linear and nonlinear mixed effects models. R package. <https://CRAN.R-project.org/package=nlme>.
- Prum, R. O., R. Torres, S. Williamson, and J. Dyck. 1999. Two-dimensional Fourier analysis of the spongy medullary keratin of structurally coloured feather barbs. *Proceedings of the Royal Society B* 266:13–22.
- R Core Team. 2020. *R: a language and environment for statistical computing*. R Foundation for Statistical Computing, Vienna.
- Revell, L. J. 2010. Phylogenetic signal and linear regression on species data. *Methods in Ecology and Evolution* 1:319–329.
- Rzeszutarski, M. S., F. L. Royer, and G. C. Gilmore. 1983. Introduction to two-dimensional Fourier analysis. *Behavior Research Methods and Instrumentation* 15:308–318.
- Symonds, M. R. E., and S. P. Blomberg. 2014. A Primer on phylogenetic generalised least squares. Pages 105–130 in L. Z. Garamszegi, ed. *Modern phylogenetic comparative methods and their application in evolutionary biology*. Springer, Berlin.
- van der Schaaf, A., and J. H. van Hateren. 1996. Modelling the power spectra of natural images: statistics and information. *Vision Research* 36:2759–2770.
- Wear, K. A. 2003. Characterization of trabecular bone using the backscattered spectral centroid shift. *IEEE Transactions on Ultrasonics, Ferroelectrics, and Frequency Control* 50:402–407.
- Xu, K. S. 2020. Spectral centroid ground motion amplitude anomaly before the Ms 8.0 Wenchuan earthquake. *Arabian Journal of Geosciences* 13:375.

Associate Editor: Nathan I. Morehouse
Editor: Erol Akçay



“It is not impossible that they breed at intervals throughout the year. This is an important point. At any rate there should be a close time on the coast of New England, during April and May, and October and November. Persons should also be fined heavily for selling lobsters with eggs attached.” From “The History of the Lobster” by A. S. Packard Jr. (*The American Naturalist*, 1874, 8:414–417).